

# RSC Advances



This is an *Accepted Manuscript*, which has been through the Royal Society of Chemistry peer review process and has been accepted for publication.

*Accepted Manuscripts* are published online shortly after acceptance, before technical editing, formatting and proof reading. Using this free service, authors can make their results available to the community, in citable form, before we publish the edited article. This *Accepted Manuscript* will be replaced by the edited, formatted and paginated article as soon as this is available.

You can find more information about *Accepted Manuscripts* in the [Information for Authors](#).

Please note that technical editing may introduce minor changes to the text and/or graphics, which may alter content. The journal's standard [Terms & Conditions](#) and the [Ethical guidelines](#) still apply. In no event shall the Royal Society of Chemistry be held responsible for any errors or omissions in this *Accepted Manuscript* or any consequences arising from the use of any information it contains.

## Synthesis of mesoporous titanium oxide for control release and high efficiency drug delivery of vinorelbine bitartrate

Gangaraju Gedda<sup>§3</sup>, Sunil Pandey<sup>§1</sup>, M Shahnawaz Khan<sup>3</sup>, Abou Talib<sup>3</sup>, Hui-Fen Wu\*<sup>1,2,3,4</sup>

<sup>1</sup>Department of Chemistry and Center for Nanoscience and Nanotechnology, National Sun Yat-Sen University, Kaohsiung, 70, Lien-Hai Road, Kaohsiung, 80424, Taiwan

<sup>2</sup>School of Pharmacy, College of Pharmacy, Kaohsiung Medical University, Kaohsiung, 807, Taiwan

<sup>3</sup>Doctoral Degree Program in Marine Biotechnology, National Sun Yat-Sen University and Academia Sinica, Kaohsiung, 80424, Taiwan

<sup>4</sup>Institute of Medical Science and Technology, National Sun Yat-Sen University, 70, Lien-Hai Road, Kaohsiung, 80424, Taiwan

Phone: +886-7-5252000-3955; Fax: +886-7-5253908

E-mail: [hwu@faculty.nsysu.edu.tw](mailto:hwu@faculty.nsysu.edu.tw) (Corresponding author: Prof. HF Wu)

§ Both authors contributed equally as the first author

---

### Abstract

The present work reports a facile method of fabrication of mesoporous titanium oxide (mTiO<sub>2</sub>) and its application for delivery of potential anticancer drug Vinorelbine bitartrate (VB) under physiological conditions. The mTiO<sub>2</sub> was functionalized with hexamethylene tetramine (HMTA), which can release formaldehyde in the acidic environment of cancer cells. Due to the nature of high porosity of mTiO<sub>2</sub>, the drug loading capacity of the mTiO<sub>2</sub>-HMTA was extremely high (about 73%) and the release of the drug was consistent for long time (about 72 hrs). The release of VB was pH dependent and found to be higher under slightly acidic condition thus mimicking cancer's environment. The role of HMTA in the present context is to trigger the release of formaldehyde under acidic condition (pH 6.5), which was responsible for killing cancer cells, while working synergistically with VB. The toxicity of the conjugate was assessed using HeLa and Vero cells. In the case of normal cells, the nano-conjugates were completely biocompatible (>75%). In vivo-toxicity was checked by staining thin slices of the tumor tissues using H&A staining. In case of tumor cells, the damage was found to be more due to inimical action of the formaldehyde.

**Key words:** Vinorelbine bitartrate, Hexamethylene tetramine, Mesoporous Titanium Oxide, HeLa cells, formaldehyde

## 1. Introduction

Delivery of chemotherapeutic payloads to solid tumors has become a daunting task due to ability of the cancer cells to auto-trigger various molecular and physiological events, which jeopardize physiological and biochemical rules of the human body<sup>1, 2</sup>. During the onset of cancer progression, the blood vessels surrounding the solid tumors get squeezed, leading to increased interstitial fluid pressure, which obstructs the delivery of most of the anti-cancer drugs<sup>3, 4</sup>. To circumvent such problems, the drug must be caged in targeted vehicles for capable of delivering the active pharmaceutical agents to solid tumors without being affected by the anatomical and physiological barriers<sup>5, 6</sup>.

One of the catastrophic consequences of the above molecular and biochemical alterations is limited diffusion and/or perfusion of oxygen (Hypoxia) due to inhomogeneous network of vascular supply, which forces the tumor physiology for rapid anaerobic shifts<sup>7</sup>. These changes lead to metabolism of glucose mainly via glycolytic instead of conventional respiration and hence accumulate lactic acids and low pH of the solid tumors<sup>8-11</sup>. Using the brighter side of hypoxia and low pH, plethora of chemotherapeutic agents have been designed which become more hostile upon interaction with the low pH regime of the cancer cells<sup>12</sup>. Certain chemical agents such as 1, 2, 4-benzotriazine 1,4-di-N-oxide (Tira pazamine, SR4233) has been demonstrated be a bio-reductive agent selectively hostile under low pH regime<sup>13</sup>. Specifically synthesized nanoparticles (NPs) is important for drug delivery due to their ability to clutch high amount of drug mainly owing to their high surface affinity<sup>14, 15</sup>, surpass the fuzzy traffic around the tumor micro-environment (depending on the shape and size)<sup>16</sup>, easy surface decoration with desired chemical moieties to make it biocompatible<sup>17-19</sup>, capable biological stimuli driven release of drug to desired target<sup>20, 21</sup> and ease for combinatorial (more than one drug) chemotherapy<sup>22</sup>. The most widely used mesoporous nano-materials are silica and carbon nanoparticles. They have gained special attention over a decade due to their extraordinary role in the controlled release of variety chemotherapeutic agents<sup>23</sup>. Mesoporous nanoparticles (MNPs) have features such as (1) high surface area and drug loading capacity (2) tunable size and shape and (3) easy modification on the external and internal surfaces, which make them ideal drug delivery vehicles<sup>24</sup>. By modifying the

surfaces of MNPs, their predestined loss as well as release of the drug can be controlled<sup>25-27</sup>. A recent addition in the list of MNPs is mTiO<sub>2</sub> NPs for delivery of therapeutics to desired targets. In a recent study, mTiO<sub>2</sub> have been fused with zirconium oxide nanoparticles and exploited as delivery of ibuprofen and their hydrolytic properties followed by structural integrity under the physiological milieu<sup>28</sup>. It has been proved to be very ideal candidate as a drug delivery vehicle.

In most of the drug delivery studies, the effect of drugs is enhanced combing them with other therapeutic moieties. In our work we have functionalized mTiO<sub>2</sub> with HMTA, a molecule that generates formaldehyde under acidic condition. Under acidic condition, its clinical efficacy has been proved in a combinatorial therapy with radiotherapy as synergistic response to induce death in cancer cells<sup>30-33</sup>. The impact of formaldehyde was found to be enormous when combined with HMTA. The results were verified using HeLa cells and histological studied (H&A staining) performed on tumor bearing mice. In this way, we have developed an efficient drug delivery vehicle capable of killing cancer cells with exceptionally high efficiency.

## 2. Materials and Methods

### 2.1. Chemicals

Vinorelbine bitartrate (VB) Titanium Chloride, Hexamethylene tetramine (HMTA), Urea and Cetyltrimmonium Bromide (CTAB) were purchased from Sigma, USA. Cells were cultured using standard conditions. MTT (2, 5-diphenyl-3-(4, 5-dimethyl-2-thiozyl) tetrazolium bromide) dimethyl sulfoxide (DMSO), were purchased from Sigma-Aldrich (St. Louis, MO, USA). HeLa cells were purchased from Bioresource culture collection center, Taiwan. Dulbecco's modified Eagle's medium was purchased from Thermo Scientific, USA (DMEM, HyClone® containing 4 mM L-glutamine, 4500 mg L<sup>-1</sup> glucose) fetal bovine serum (FBS) were purchased from Gibco, USA. Phosphate buffer saline (PBS), trypsin-EDTA solution (17,000 U/l trypsin mixed with 0.2 g L<sup>-1</sup> EDTA) and pen-strep solution (10000 U/mL penicillin mixed with 10 mg / mL streptomycin) were purchased from Lonza, Belgium.

## 2.2. Characterization of the nanoparticles

For Transmission Electron Microscopy (JEOL, Japan) analysis, samples were coated on to copper grid and dried overnight at 60 °C. X-ray diffraction (Bruker, Germany) was performed using dried powder of the mTiO<sub>2</sub> NPs. Fourier transform infrared spectroscopy, Bruker, Germany) was performed to assess the conjugation of nanoparticles with other moieties. The quantitation of the drug was done by using calibration curve assisted by UV-Vis Spectroscopy (Thermo Evolution, USA).

## 2.3. Evaluation of the drug encapsulation studies

Drug encapsulation efficiency (DLE) of the mTiO<sub>2</sub> nanoparticles was calculated using following equation:

$$DLE = \frac{\text{Theoretical amount of drug loaded} - \text{Free drug}}{\text{Theoretical amount of drug loaded}} \times 100 \dots\dots\dots (1)$$

The quantification of the drug was done using calibration curve by UV-Visible spectroscopy at 325 nm

## 2.4. In vitro drug release Studies

Cumulative release of the drug was calculated as follows:

$$\%CR = \frac{C_{0-t}}{C_0} \times 100 \dots\dots\dots(2)$$

Where, C<sub>0</sub> is the initial concentration and C<sub>0-t</sub> is the final concentration.

8mL of post-dialyzed mTiO<sub>2</sub>-VB conjugate was filled in dialysis membranes (2 kDa, Spectrum Labs, USA) and kept for dialysis against deionized water at pH 6.5 and 7.2. At regular interval of time, the quantity of the drug released was calculated spectroscopically at 325 nm.

## 2.5. Culturing animal cells and their interaction with nanoparticles

HeLa (human epithelial cervical cancer) and Vero cells were cultured in DMEM under humid conditions in CO<sub>2</sub> incubator at 37 °C for 24 hrs till the confluence reached to ~75%.

The cells were incubated in 96 well plates and allowed to grow under optimum conditions for 24 hrs. Different concentrations of mTiO<sub>2</sub>, HMTA, mTiO<sub>2</sub>-HMTA, mTiO<sub>2</sub>-HMTA and VB alone were added in the well after ensuring the sufficient growth. The cyto-toxicity of the nano-conjugates was done using standard MTT assay. 250µg mL<sup>-1</sup> MTT was added in the cells containing nano-conjugates and incubated for 2 hrs. Colored complex was replaced with DMSO and measured spectroscopically at 570 nm.

### 2.6. *In-vivo* toxicity

Healthy ICR nude mice (Lasco, Charles River Technology, Taiwan, 20-22 grams) were maintained in ideal conditions at ambient temperature. The experiment was performed to follow the ethical rules of National Sun Yat-Sen University, Taiwan. The tumor was induced by injecting A549 cells (~ 106 cells/ml) along with Hanks Balanced salt solution in the right flank of mice. The mice were observed for tumor growth and the subsequent experiments were planned accordingly. The mice were divided in two groups, which were injected with mTiO<sub>2</sub>-HMTA-VB conjugate and phosphate buffer saline. The therapeutic dose of the drug was kept to be 25 mg kg<sup>-1</sup>. In order to check the organ specific toxicity of the mTiO<sub>2</sub>-HMTA-VB conjugate, the mice was euthanized using standard methods and organs were removed to make wax embedded cake. Thin sections were made using microtome and stained using hematoxylin/eosin (H&E). The slices were observed under inverted microscopy. The weight of the mice was also recorded for 45 days and compared with control.

## 3. Results and discussions

### 3.1. *Synthesis and characterization of mTiO<sub>2</sub>*

The mTiO<sub>2</sub> was prepared using thermolytic method involving urea as reducing agent and CTAB as template to prepare the mesoporous NPs<sup>34, 35</sup>. The advantage of porosity in the present contest is to enhance the drug loading capacity for delivery of therapeutic amount of drugs. This method is simple and reproducible for fabrication of mTiO<sub>2</sub> due to the involvement of urea as shape-navigating molecules.

The UV-Vis spectra of mTiO<sub>2</sub> and its nano-conjugates are displayed in fig.1. In the case of aqueous bare mTiO<sub>2</sub>, a sharp peak at 450 nm was observed in the UV spectra (Inset fig. 1). After anchoring HMTA onto the surface of bare mTiO<sub>2</sub>, the peaks were shifted to 385 nm (blue shift of ~75 nm), which indicates the molecular interaction of HMTA with mTiO<sub>2</sub>

surface. A stark change was observed after the attachment of VB with on mTiO<sub>2</sub>-HMTA conjugate. There were some significant optical changes after attaching the drugs on the above conjugate, decrease in the intensity followed by emergence of two peaks at 370 nm and 335 nm. The peak at 335 nm is a signature marker of anti-neoplastic drug VB. With respect to UV spectra of bare VB (~325 nm) the nano-conjugates were found to have altered optical properties. These observations were considered to be primary observation confirming the interactions between them.

The surface interaction of the mTiO<sub>2</sub> with other conjugates is shown in fig. 2. FTIR spectrum of the HMTA capped mTiO<sub>2</sub> nanostructures collected in the range of 4000–450 cm<sup>-1</sup> are shown in Fig. 2(a). The broad band located at 500 cm<sup>-1</sup> is the typical characteristic band of Ti–O vibrational band<sup>36</sup>. The band at 3448 cm<sup>-1</sup> and 1636 cm<sup>-1</sup>, 1622 cm<sup>-1</sup> is correlated to N–H mode of stretching and bending vibrations. The peaks at 1111 cm<sup>-1</sup> are corresponding C–C bending vibration. The bands at 1460 cm<sup>-1</sup>, 1390 cm<sup>-1</sup> and 900–600 cm<sup>-1</sup> ranges are corresponding to C–H bending vibrations. These functional groups confirmed presence of HMTA on the surface of nanoparticles.

The FTIR spectrum of the VB-HMTA capped mTiO<sub>2</sub> complex nanostructures is shown in Fig. 2(b). It can be clearly seen that there are few additional bands. The bands at 2955 cm<sup>-1</sup> and 2864 cm<sup>-1</sup> are corresponding to –CH<sub>3</sub>, –CH<sub>2</sub>, –C–H stretching vibration in VB. The weak band at 1745 cm<sup>-1</sup> belongs to –COOH group. These functional groups are conforming that the presence of VB. Fig. 2(c) displays the bare mTiO<sub>2</sub> NPs IR spectrum. The absorption band around at 1657 cm<sup>-1</sup> and 1649 cm<sup>-1</sup> was caused by a bending vibration of correspond to the surface adsorbed water and hydroxyl groups. The peak centered at ~1046 cm<sup>-1</sup> due to characteristic O – O stretching vibration. The sharp peak at 1450 cm<sup>-1</sup> can be attributed to the lattice vibrations of TiO<sub>2</sub>. The band at 664 cm<sup>-1</sup> is due to titanium oxide and assigned to the stretching of Ti–O–Ti.

TEM image (Fig. 3a and b) shows the monodispersed spherical mTiO<sub>2</sub> and size ranging from 10 - 50 nm with maximum nanoparticles in 30 nm regime. This is also evident from as the histogram (Inset of fig. 3a). Smaller size (~30 nm) is ideal for drug delivery because it escapes the rapid vascular clearance after entering in the tumor regime. Fig. 3c explains the SEAD pattern of nanoparticles confirming it to be crystalline in nature. The diffraction of the X-rays through different atomic planes can be clearly seen in the pattern. X-ray diffraction

plot of the  $m\text{TiO}_2$  is explained in fig. 3d. The Bragg's diffraction patterns explain the presence of anatase phases in the structures. The corresponding angles and their specification are highlighted in fig. 3d.

### 3.2. *In-vitro drug release studies*

The efficiency of  $m\text{TiO}_2$  as an efficient drug vessel was assessed on the basis of drug loading capacity as well as the release pattern of the VB at specified pH values (pH 7.2 and 6.5). The drug loading capacity of the as synthesized nanoparticles was found to be 75% (using Eq.1), which falls within the acceptable range of most of the drug delivery vehicles. Obviously, the high drug loading capacity is due to high porosity of the NPs used as drug delivery vehicle. The  $m\text{TiO}_2$  NPs were confirmed an excellent drug delivery vehicles to catalyze/control the pH dependent release of the drugs (Fig. 4). At physiological pH, 48% of free VB was fired in 24 hrs; in a stark contrast to VB anchored to  $m\text{TiO}_2$  is 34.78% in 60 hrs (Fig. 4a). This explains the contention of the nano-vessel as an ideal carrier of chemotherapeutic agents. Due to the porous nature of the  $m\text{TiO}_2$  nanoparticles, high amount of drug (75%, calculated by using Eq.1) was incorporated and hence the release was found to be for substantial amount of time. Another peculiar feature of drug release was found to be rapid firing of VH at lower pH regime (pH 6.4), with respect to free VB (88% in 24 hrs);  $m\text{TiO}_2$ -HMTA-VH conjugate fired 78 % in 60 hrs (Fig. 4b). The advantage of drug release at lower pH regime deserves special attention. During the cancer transformation, the pH of the tumor microenvironment becomes acidic due to acid catalyzed biochemical reactions<sup>37,38</sup>. Thus, the sustained release at this pH helps to enhance the efficacy of the cancer chemotherapy.

### 3.3. *HMTA mediated cyto-toxicity*

This section explains the exceptional capacity of  $m\text{TiO}_2$ -HMTA-VB complex to release formaldehyde at lower pH. As explained in earlier sections, formaldehyde works potentially against cancer cells<sup>39</sup>. In combination of radiotherapy, HMTA has been used to enhance the overall impetus of the process<sup>30</sup>. However, the key role is only played by lower pH regime and the release of formaldehyde is not dependent on radiotherapy. Figure 5 displays the toxicity of various nano-conjugates. All experiments were performed in triplicates with  $SD=1.45$ ,  $p<0.05$ . In order to prove the impact of nano-conjugates, Vero and HeLa cell lines were used. As shown in figure, the  $m\text{TiO}_2$  and HMTA alone exert mild hostile impact on the Vero, thus the survival rate was found to be 76% and 54% at  $1\mu\text{g/ml}$  respectively. On Vero

cells the effect of VB, TiO<sub>2</sub>-HMTA and mTiO<sub>2</sub>-HMTA-VB was found to be 47,56.8 and 43% respectively. However, on HeLa cells the impact of mTiO<sub>2</sub>, HMTA, mTiO<sub>2</sub>-HMTA and mTiO<sub>2</sub>-HMTA-VB was found to be 60, 58.4, 47, 38 and 20% respectively. The interesting aspect was found in case of mTiO<sub>2</sub>-HMTA-VB (20% at highest concentration) due to formation of formaldehyde under acidic pH. This unlocks another feature of the mTiO<sub>2</sub>-HMTA-VB as dual-pronged weapon to target cancer cells by synergistic effect of VB, formaldehyde release at lower pH regime tumor microenvironment. HMTA has been investigated in detail for their ability to release formaldehyde<sup>39</sup>.

### 3.4. *In vivo* toxicity

Fig. 6 is the representation of *in vivo* toxicity after injection of the drugs along with the drug delivery vehicles. The impact of drugs on the health of the mice is explained in terms of the body weight over a stipulated period of the time. Untreated mice body weight slightly increases day by day which have achieved 10% increase on 40<sup>th</sup> day. The mTiO<sub>2</sub>-HMTA-VB complex treated group body weight slightly decreases until it is reached to 10%. Beside this VB treated shows significant decreased of body weight (20%). The conjugates were compared with the control and found to be fairly non-toxic.

### 3.5. *Histological study*

Histological examination reveals effect of drug and other nano-conjugate on vital organs of experimental mice models.. After 15 h of injecting 20 µg mL<sup>-1</sup> of mTiO<sub>2</sub>-HMTA-VB in mice, the necrosis studies were performed for important organs such as heart, liver, and kidney. Organs were sliced into sections by using the Microtomy. Further, the tissues were stained with Haematoxylin and Eosin dye. After the treatment, mice organs tissue sections were observed under microscope. Fig. 7 a, b and c are tissue section of heart, liver and kidney respectively in which PBS was injected as a control. It can be seen that intactness of membranes of cells are maintained<sup>37</sup>. Whereas, mice treated by mTiO<sub>2</sub>-HMTA-VB (Fig. 7 d,e and f) show some lesion or abnormality in their plasma membrane in histological tissue section. Some cells became black may be due to necrosis. It can be inferred by examining tissue sections of organs that mTiO<sub>2</sub>-HMTA-VB did not show major toxic effect on vital organs.

Figs. 8 (a and b) display stained sections of both tumors, control and treated by HMTA, show undamaged periphery of tissues. Although, some cells were died in the case of HMTA,

as it released formaldehyde and ammonia<sup>30-33</sup>. Whereas, tumor, which was treated by VB, show greater inimical effect, as it damage more tissue, which can be seen as a dark spot inside tissue section (Fig. 7c). Tumor, which was treated by mTiO<sub>2</sub>-HMTA-VB shown remarkable positive result, and the vascular tissue near the periphery were damaged, increased dark spots inside tissue shows the death of many cells. According to Marty M et al VB interact with tubulin during the mitosis stage, which leads to death of tumor cells and inhibits further vascularization<sup>40, 41</sup>. The *in vivo* toxicity results reveal the inimical effect of formaldehyde generated by HMTA under hypoxic condition (Fig. 8). Under hypoxic condition, the low pH generated by typical reaction involving pyruvic acid, HMTA release formaldehyde, which is toxic to cancer cells. Formaldehyde kills cells by irreversible cross-linkage of primary amines with adjacent cells, thereby hampering cellular metabolism.

#### 4.4. Conclusion

Mesoporous titanium oxide synthesized using thermolytic methods was proved be an efficient drug delivery system having high drug loading capacity. The role of HMTA was found to be the key factor in killing the cancer cells in synergistic action with Vinorelbin bitartrate under low pH regime. The function of HMTA is responsible for the release of formaldehyde under acidic condition. The nano-conjugates were highly biocompatible under *in vitro* and *in vivo* conditions.

#### Acknowledgement

We thank financial support from ministry of science and technology (MOST) of Taiwan.

#### Notes

The authors declare no competing financial interest.

#### Figure captions.

**Figure 1:** UV-Vis spectroscopy of conjugates involved in reaction (a) mTiO<sub>2</sub> (b) mTiO<sub>2</sub> – HMTA (c) mTiO<sub>2</sub>-HMTA-VB. Inset shows the magnified view UV-Visible Spectroscopy of mTiO<sub>2</sub>

**Figure 2:** TEM image of (a and b) mTiO<sub>2</sub> displaying the size ranging from 40-50 nm (Inset

of a display histogram of size) (c) SEAD pattern and (d) XRD of mTiO<sub>2</sub>

**Figure 3:** FTIR of (a) mTiO<sub>2</sub> (b) mTiO<sub>2</sub>-HMTA and (c) mTiO<sub>2</sub>-HMTA-VB showing the Interaction chemistry among nanoparticles

**Figure 4:** pH dependent in vitro vinorelbine bitartrate release profile at (a) pH=7.2 (b) pH=6.4

**Figure 5:** Cytotoxicity analysis of the nano-conjugates on HeLa (a) and Vero (b) cells (n=3, p<0.05)

**Figure 6:** *In vivo* toxicity of the nano-conjugates on experimental mice model (n=3, p<0.05)

**Figure 7:** Tissue section of vital organs (stained by Haemotoxolin and Eosin) of heart, liver, and kidney were treated by PBS (a) heart (b) Kidney and (c) Liver (upper panel) and lower panel shows (d) heart (e) Kidney and (f) Liver treated by mTiO<sub>2</sub>-HMTA-VB.

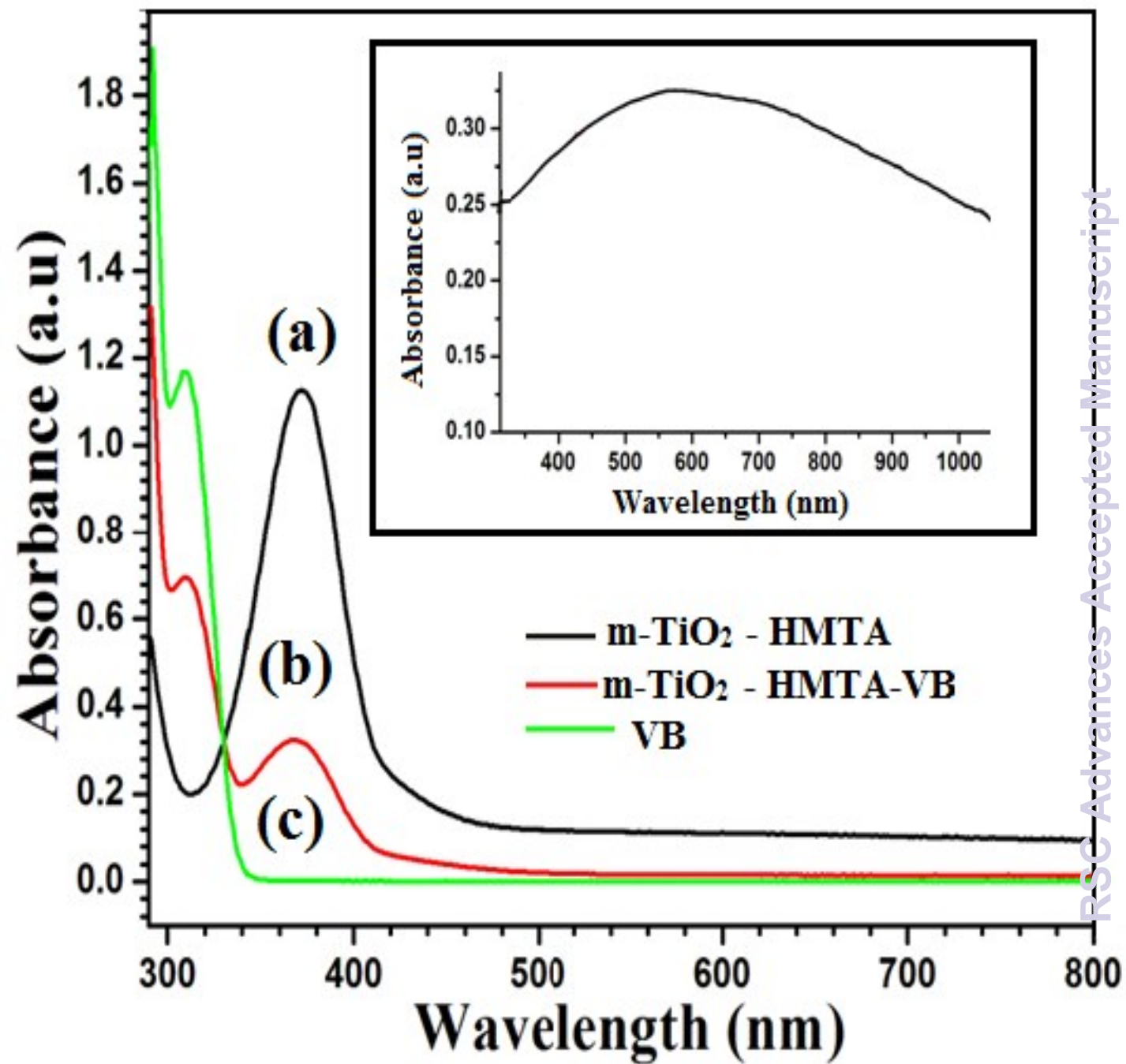
**Figure 8:** Histological Examination of tumor tissues after injection of the (a) PBS, (b) VB and (c) mTiO<sub>2</sub>-HMTA-VB Nano-conjugates.

## References:

1. G. A. Koning, A. M. Eggermont, L. H. Lindner and T. L. ten Hagen, *Pharmaceutical research*, 2010, 27, 1750-1754.
2. D. Y. Furgeson, M. R. Dreher and A. Chilkoti, *Journal of Controlled Release*, 2006, 110, 362-369.
3. R. K. Jain and T. Stylianopoulos, *Nature reviews clinical oncology*, 2010, 7, 653-664.
4. F. Danhier, O. Feron and V. Pr at, *Journal of Controlled Release*, 2010, 148, 135-146.
5. O. C. Farokhzad and R. Langer, *ACS nano*, 2009, 3, 16-20.
6. K. Cheng, S. Peng, C. Xu and S. Sun, *Journal of the American Chemical Society*, 2009, 131, 10637-10644.
7. J. Brown, *The British journal of radiology*, 1979, 52, 650-656.
8. G. Helmlinger, F. Yuan, M. Dellian and R. K. Jain, *Nature medicine*, 1997, 3, 177-182.
9. C. W. Song, H. Park and B. D. Ross, in *Antiangiogenic Agents in Cancer Therapy*, Springer, 1999, pp. 51-64.
10. R. Becelli, G. Renzi, R. Morello and F. Altieri, *Journal of Craniofacial Surgery*, 2007, 18, 1051-1054.
11. J. G. Rhee, T. H. Kim, S. H. Levitt and C. W. Song, *International Journal of Radiation Oncology\* Biology\* Physics*, 1984, 10, 393-399.
12. J. M. Brown and W. R. Wilson, *Nature Reviews Cancer*, 2004, 4, 437-447.
13. L. H. Gray, A. D. Conger, M. Ebert, S. Hornsey and O. Scott, *The British journal of radiology*, 1953, 26, 638-648.
14. S. Pandey, G. Oza, A. Mewada, R. Shah, M. Thakur and M. Sharon, *Journal of Materials Chemistry B*, 2013, 1, 1361-1370.
15. B. D. Chithrani, A. A. Ghazani and W. C. Chan, *Nano letters*, 2006, 6, 662-668.
16. H. I. Labouta and M. Schneider, *International journal of pharmaceutics*, 2010, 395, 236-242.
17. W. Qin, D. Ding, J. Liu, W. Z. Yuan, Y. Hu, B. Liu and B. Z. Tang, *Advanced Functional Materials*, 2012, 22, 771-779.

18. X. Zhang, X. Zhang, S. Wang, M. Liu, L. Tao and Y. Wei, *Nanoscale*, 2013, 5, 147-150.
19. D. Li, H. Sun, L. Jiang, K. Zhang, W. Liu, Y. Zhu, J. Fangteng, C. Shi, L. Zhao and H. Sun, *ACS applied materials & interfaces*, 2014.
20. J. Cheng, B. A. Teply, I. Sherifi, J. Sung, G. Luther, F. X. Gu, E. Levy-Nissenbaum, A. F. Radovic-Moreno, R. Langer and O. C. Farokhzad, *Biomaterials*, 2007, 28, 869-876.
21. F. Mou, C. Chen, Q. Zhong, Y. Yin, H.-R. Ma and J. Guan, *ACS applied materials & interfaces*, 2014.
22. O. C. Farokhzad, J. Cheng, B. A. Teply, I. Sherifi, S. Jon, P. W. Kantoff, J. P. Richie and R. Langer, *Proceedings of the National Academy of Sciences*, 2006, 103, 6315-6320.
23. D. Avnir, T. Coradin, O. Lev and J. Livage, *Journal of Materials Chemistry*, 2006, 16, 1013-1030.
24. Y. Wang and F. Caruso, *Chemistry of materials*, 2006, 18, 4089-4100.
25. J. Huang, I. Ichinose and T. Kunitake, *Angewandte Chemie International Edition*, 2006, 45, 2883-2886.
26. Y. G. Mishael, P. L. Dubin, R. de Vries and A. B. Kayitmazer, *Langmuir*, 2007, 23, 2510-2516.
27. E. H. Otal, P. C. Angelomé, S. A. Bilmes and G. J. Soler-Illia, *Advanced Materials*, 2006, 18, 934-938.
28. X. Wang, D. Chen, L. Cao, Y. Li, B. J. Boyd and R. A. Caruso, *ACS applied materials & interfaces*, 2013, 5, 10926-10932.
29. S.-i. Masunaga, K. Ono, H. Hori, M. Akaboshi, K.-i. Kawai, M. Suzuki, Y. Kinashi, S. Kasai, H. Nagasawa and Y. Uto, *Radiation medicine*, 1997, 16, 441-448.
30. S. Masunaga, K. Tano, M. Watanabe, G. Kashino, M. Suzuki, Y. Kinashi, K. Ono and J. Nakamura, *Evaluation*, 2009, 82.
31. S.-i. Masunaga, K. Tano, J. Nakamura, M. Watanabe, G. Kashino, A. Takahashi, H. Tanaka, M. Suzuki, K. Ohnishi and Y. Kinashi, *Journal of radiation research*, 2010, 51, 27-35.
32. E. A. Cohen Hubal, P. M. Schlosser, R. B. Conolly and J. S. Kimbell, *Toxicology and applied pharmacology*, 1997, 143, 47-55.
33. S.-I. Masunaga, K. Tano, J. Nakamura, M. Watanabe, G. Kashino, M. Suzuki, Y. Kinashi and K. Ono, *Experimental and therapeutic medicine*, 2010, 1, 169-174.
34. M. Sharon, N. Sundarakoteeswaran, P. Kichambare, M. Kumar, Y. Ando and X. Zhao, *Diamond and related materials*, 1999, 8, 485-489.
35. M. Sharon, S. Jain, P. Kichambare and M. Kumar, *Materials chemistry and physics*, 1998, 56, 284-288.
36. M. Wan, W. Li, Y. Long and Y. Tu, *Anal. Methods*, 2012, 4, 2860-2865.
37. M S Khan, S. Pandey, A. Talib, H-FWu. Controlled delivery of dopamine hydrochloride using surface modified carbon dots for Neuro diseases. *Colloids and Surfaces B: Biointerfaces* 2015, 134, 140-146
38. P. Vaupel, F. Kallinowski and P. Okunieff, *Cancer research*, 1989, 49, 6449-6465.
39. R. B. Conolly, J. S. Kimbell, D. Janszen, P. M. Schlosser, D. Kalisak, J. Preston and F. J. Miller, *Toxicological Sciences*, 2004, 82, 279-296.
40. V. Dieras, J. Extra, E. Bellissant, M. Espie, F. Morvan, J. Pierga, L. Mignot, P. Tresca and M. Marty, *Journal of clinical oncology*, 1996, 14, 3097-3104.
41. M. Marty, J. Extra, V. Dieras, S. Giacchetti, S. Ohana and M. Espie, *Drugs*, 1992, 44, 29-35.

Figure. 1



RSC Advances Accepted Manuscript

Figure. 2

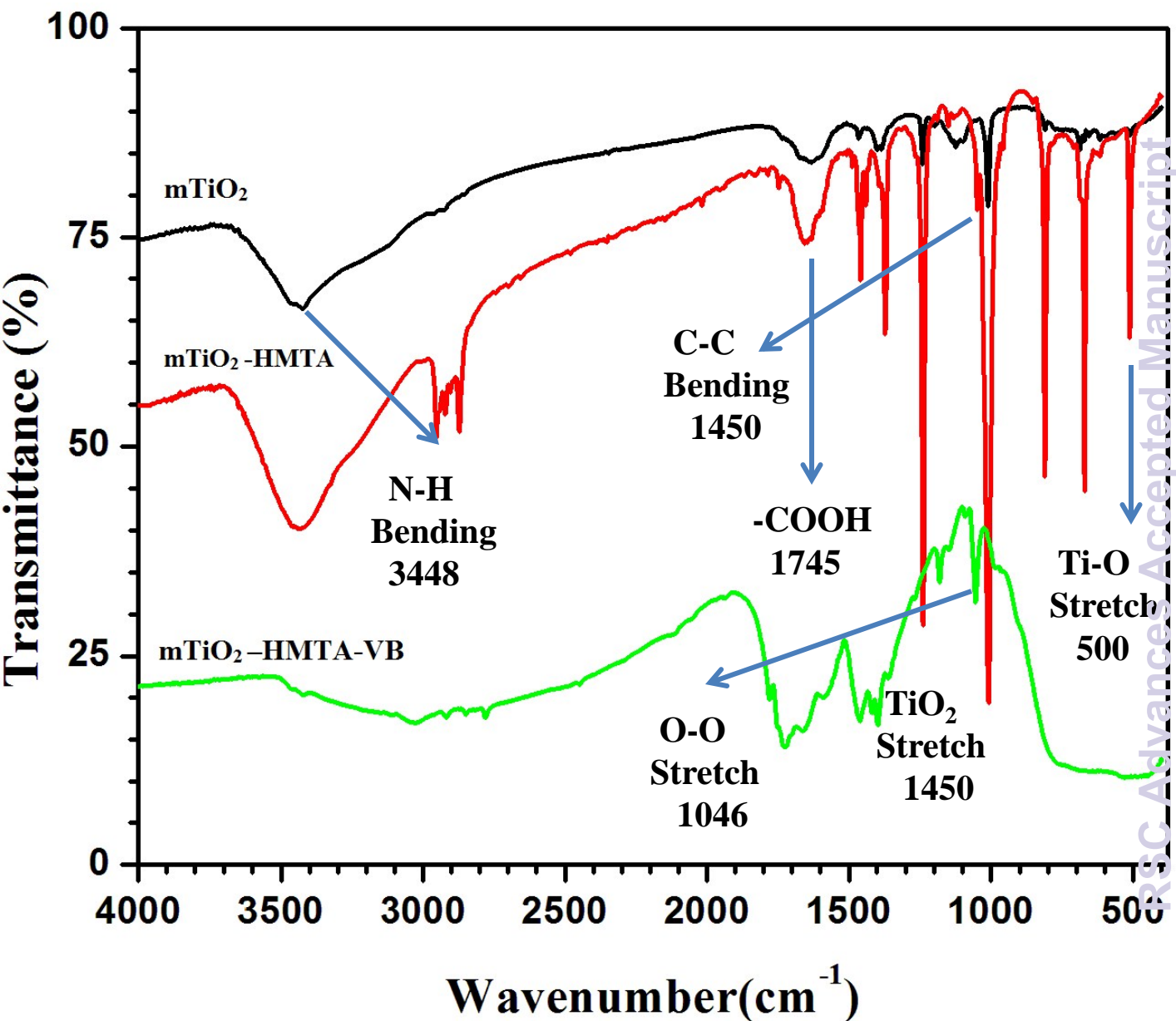
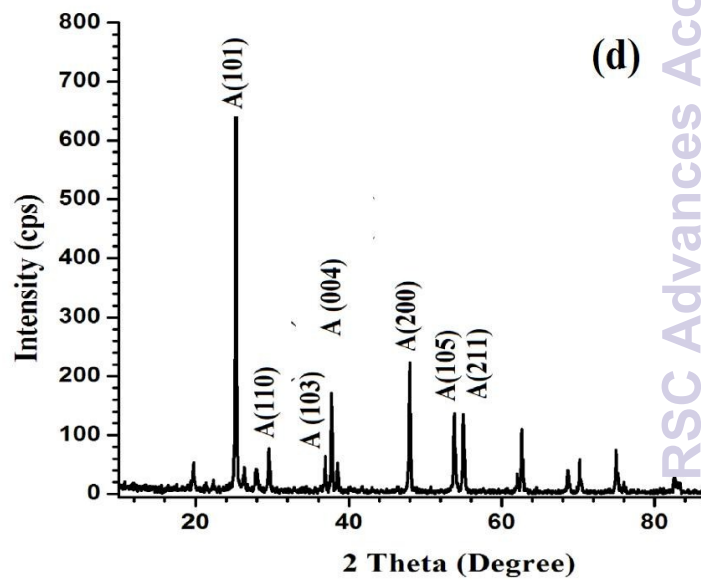
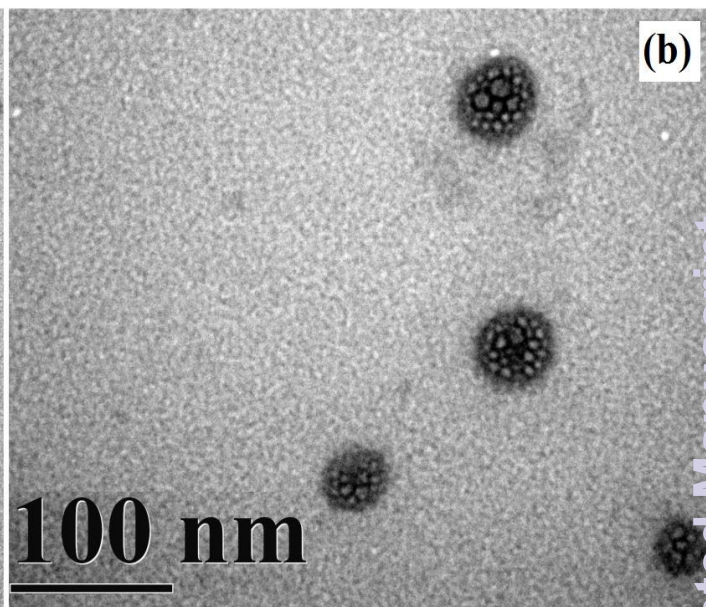
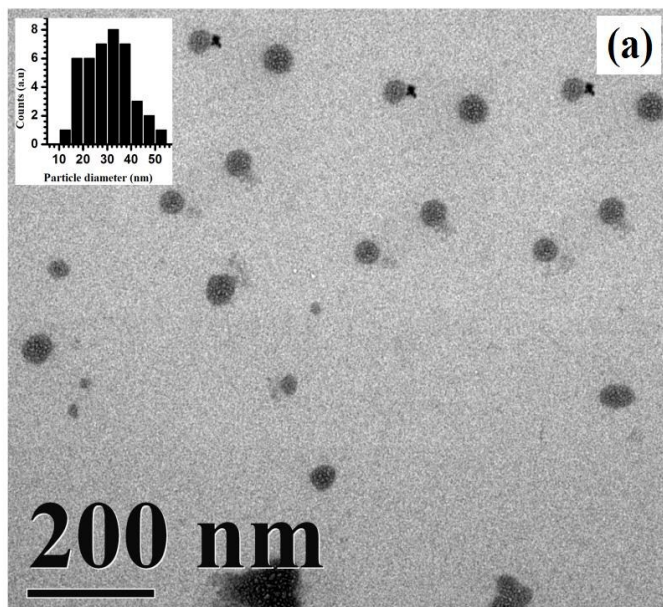


Figure. 3



RSC Advances Accepted Manuscript

Figure. 4

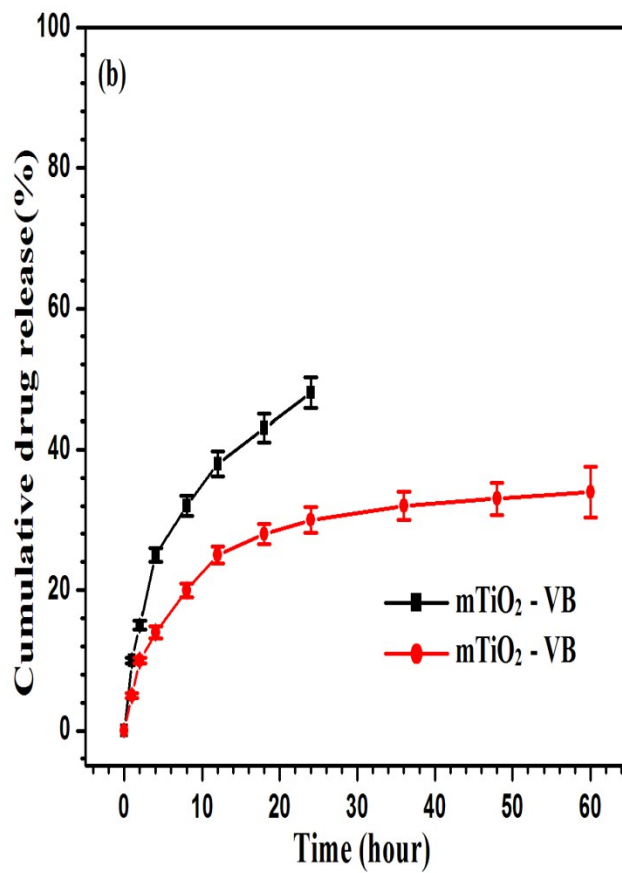
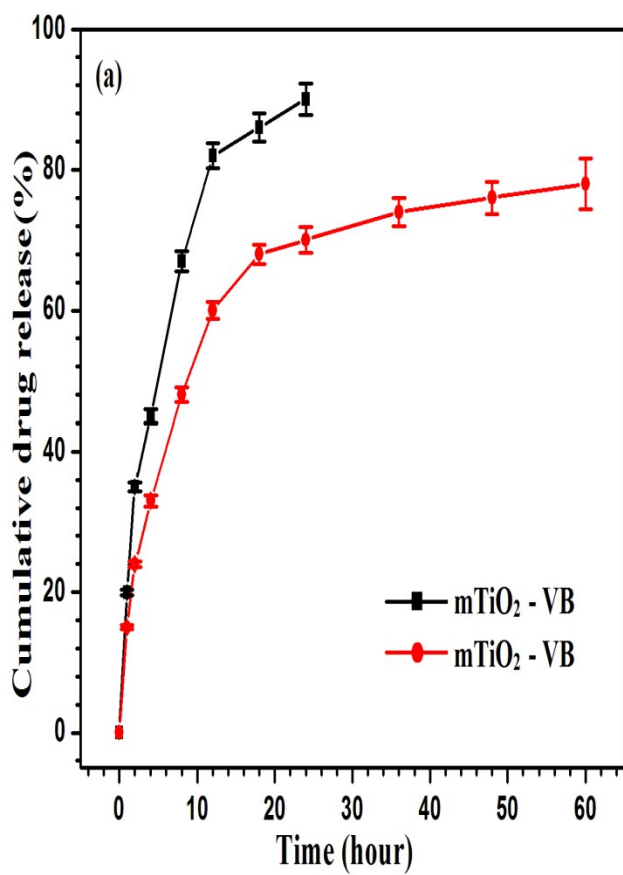


Figure. 5

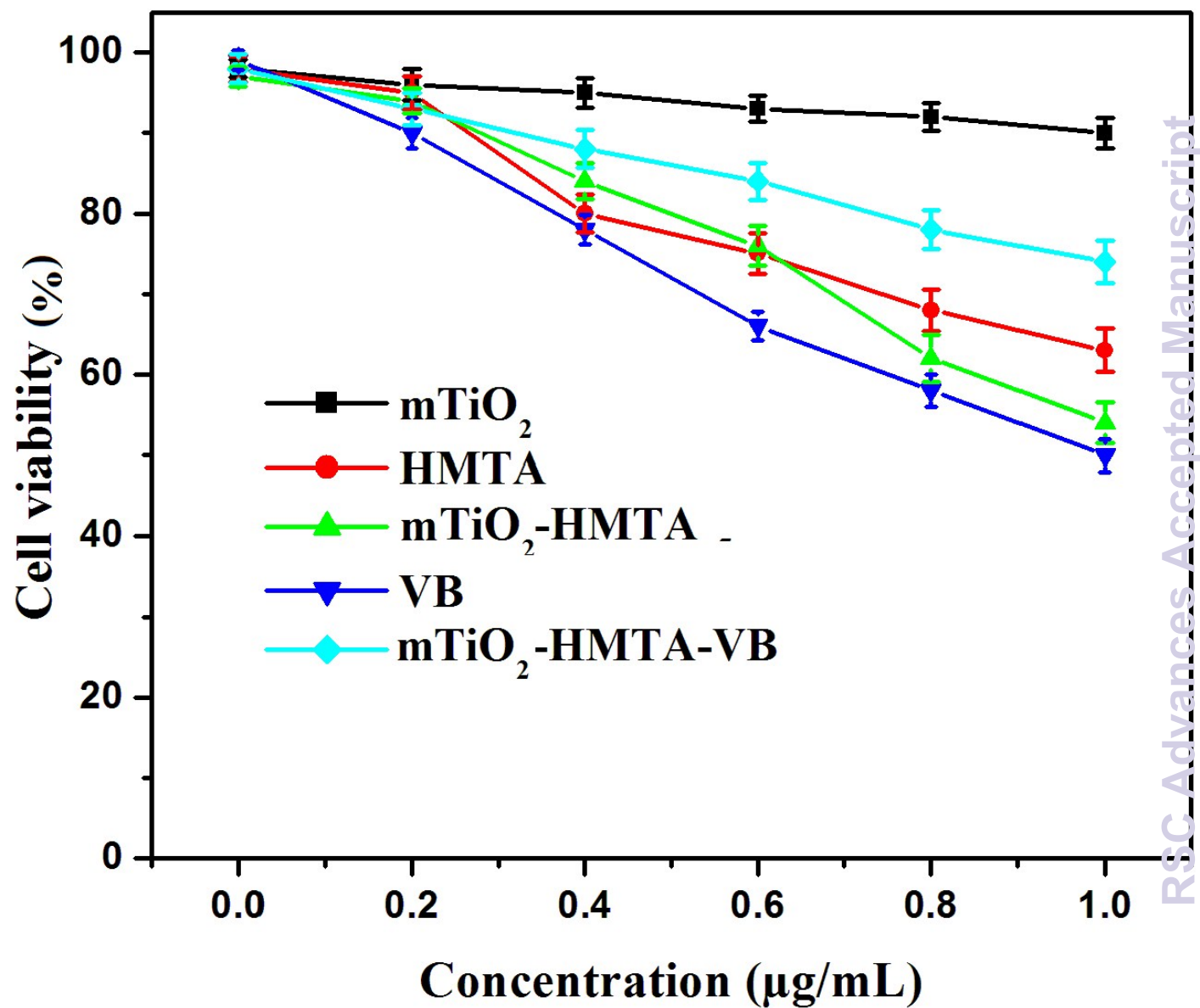
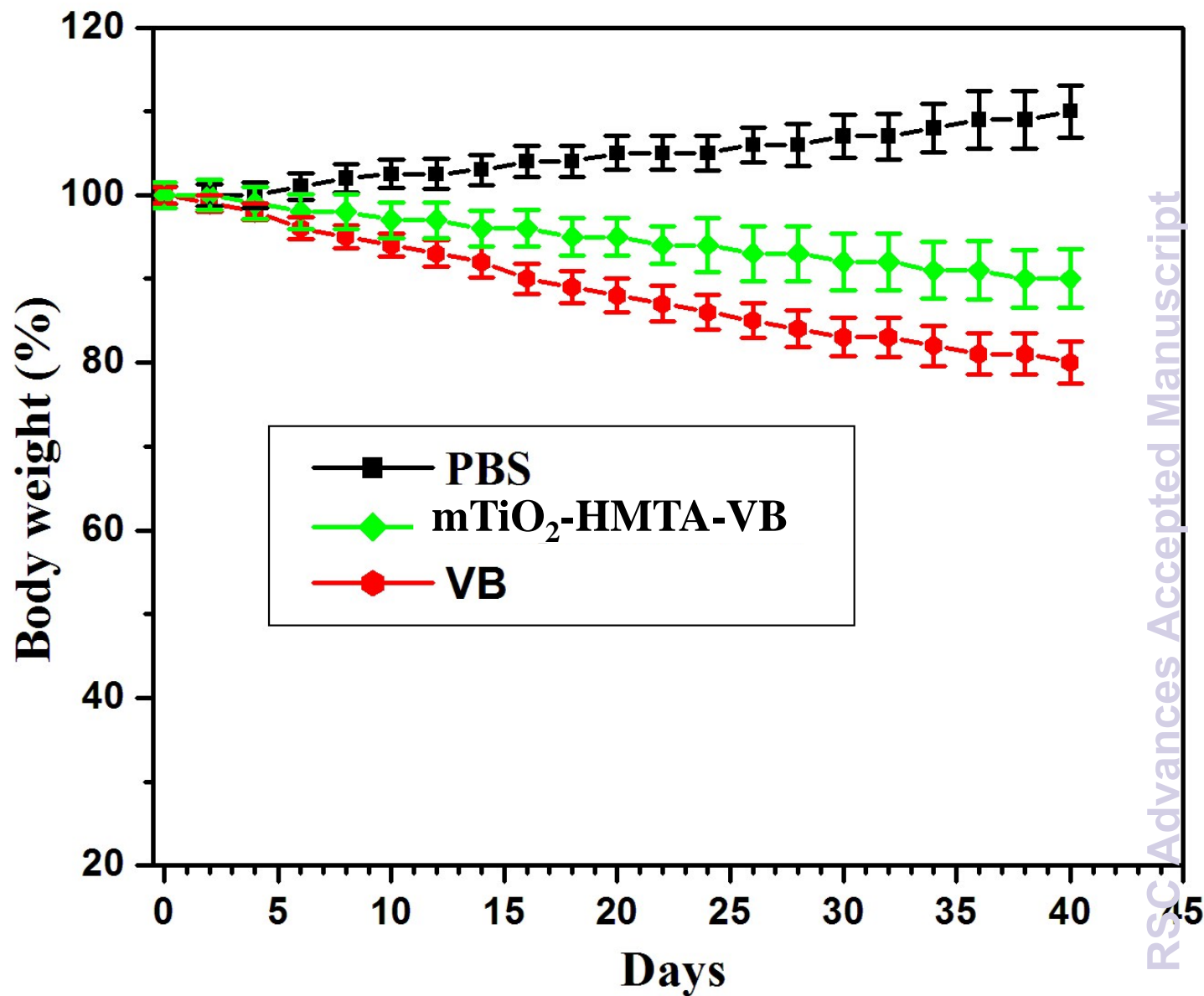
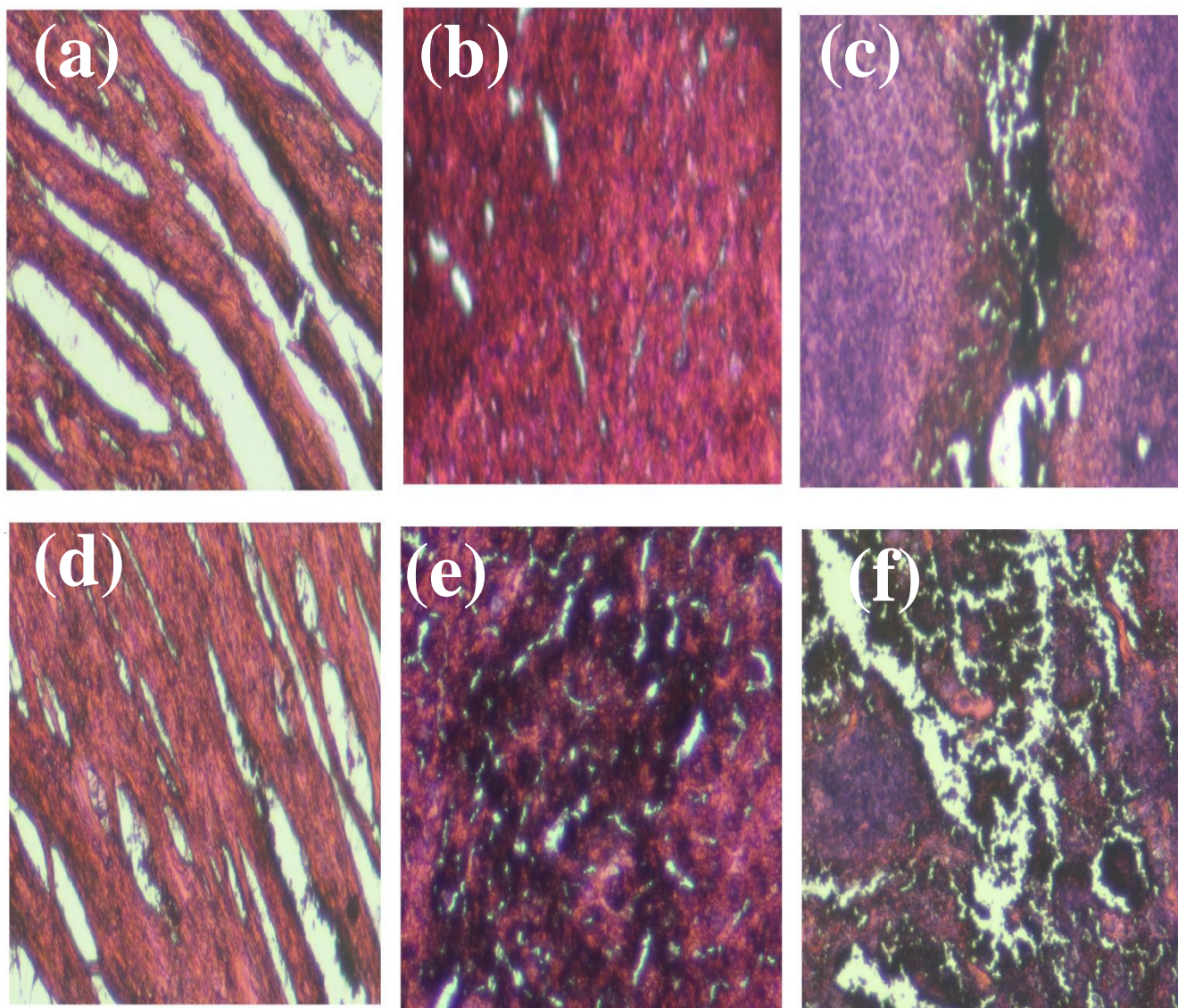
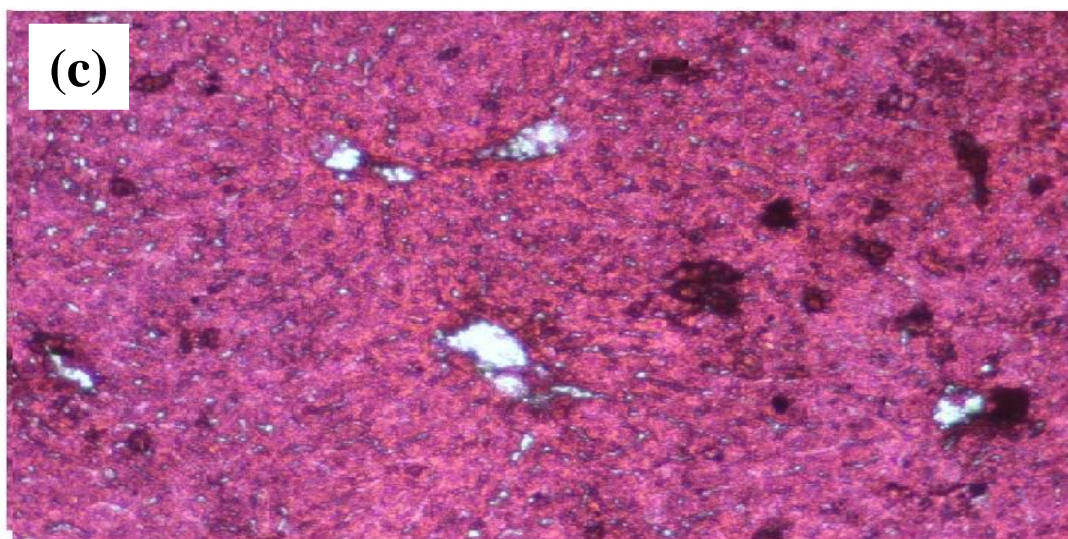
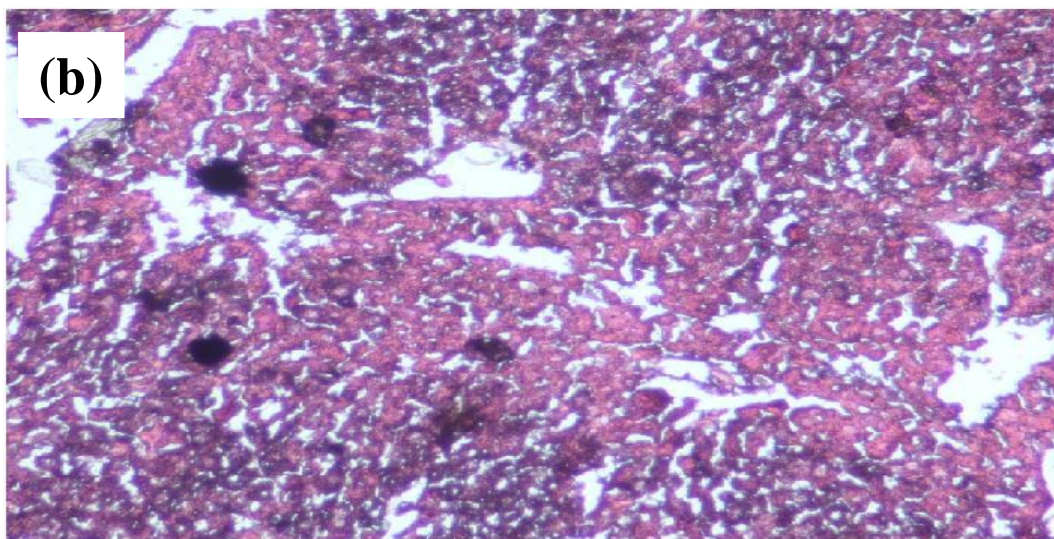
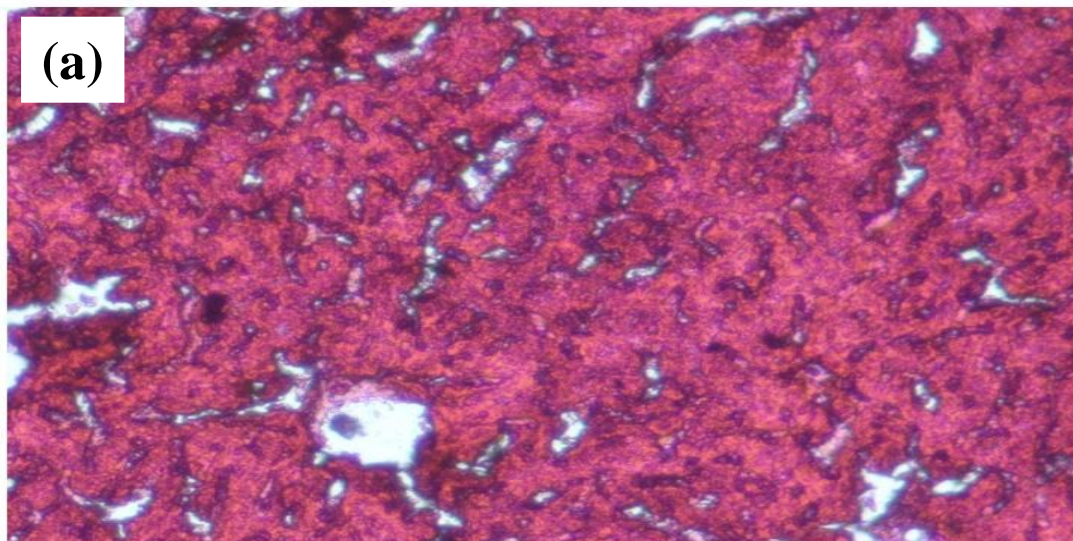


Figure. 6



**Figure. 7**

**Figure. 8**



## Schematic illustration of porous titanium oxide for drug delivery of vinorelbine bitartrate

